C. R. Mecanique 343 (2015) 645–655

Contents lists available at ScienceDirect

Comptes Rendus Mecanique

www.sciencedirect.com

Acoustic metamaterials and phononic crystals

Acoustic coatings for maritime systems applications using resonant phenomena

Pierre Méresse [a,*], Christian Audoly [a], Charles Croënne [b], Anne-Christine Hladky-Hennion [b]

[a] DCNS Research, CEMIS, BP 403 (Le Mourillon), 83055 Toulon cedex, France
[b] IEMN (UMR 8520 CNRS), ISEN Department, 41, boulevard Vauban, 59046 Lille cedex, France

ARTICLE INFO

Article history:
Received 8 April 2015
Accepted 9 July 2015
Available online 29 July 2015

Keywords:
Acoustic coatings
Underwater acoustics
Resonant phenomena

ABSTRACT

There is a great interest in the availability of acoustic coatings for maritime systems applications, in particular for the reduction of radiated noise in water. The purpose of this paper is to give an overview of recent results regarding the design of such materials, which are classically of two main types: the micro-inclusion technology and the Alberich-type coating. In both cases, resonances of inclusions are exploited. Here, the concepts are extended to configurations with several layers of periodic arrangements of soft and rigid inclusions. The analysis is done using the finite-element technique. The results show a wide variety of acoustical phenomena, allowing us to customise the design according to different applications.

© 2015 Académie des sciences. Published by Elsevier Masson SAS. All rights reserved.

1. Introduction

1.1. Acoustic coatings in maritime applications

In the context of naval operations, passive and active sonar systems are commonly used to detect ships or submarines using acoustic wave propagation and signal processing. One of the most efficient technological solutions to reduce the threats is the use of hull external acoustic coatings, mainly of two types [1], as shown in Fig. 1:

- decoupling coatings consisting in surrounding the radiating parts of the hull by a layer of compliant material. The role of a decoupling coating is to reduce the radiation factor, or radiation efficiency, of the hull;
- anechoic coatings, whose role is to reduce acoustic reflection from the hull, by absorbing incoming waves.

We must also stress that there is currently an increasing concern about the protection of marine life regarding underwater sound emitted by human activity at sea. Indeed, the Maritime Strategy Framework Directive adopted in 2008 by the European Union [2] requires that the member states ensure a good environmental status in European maritime areas, including the introduction of energy, underwater noise being one of these. As a consequence, the reduction of underwater

* Corresponding author.
E-mail addresses: pierre.meresse@gmail.com (P. Méresse), christian.audoly@dcnsgroup.com (C. Audoly), anne-christine.hladky@isen.fr (A.-C. Hladky-Hennion).

http://dx.doi.org/10.1016/j.crme.2015.07.004
1631-0721/© 2015 Académie des sciences. Published by Elsevier Masson SAS. All rights reserved.

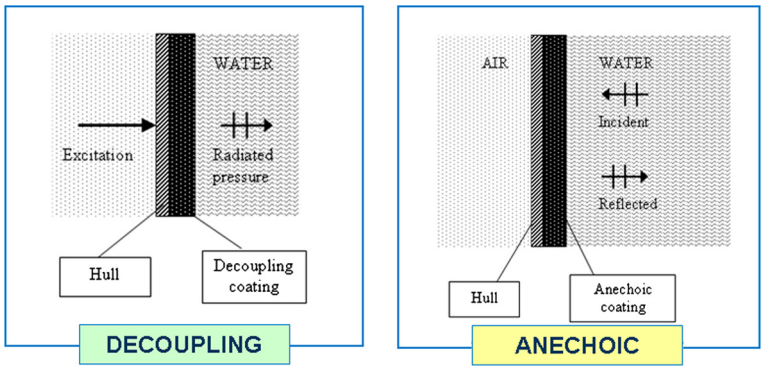

Fig. 1. (Colour online.) The two main types of acoustic hull coatings: (on the left) decoupling coating and (on the right) anechoic coating.

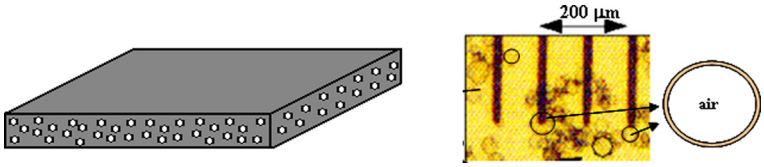

Fig. 2. (Colour online.) (On the left.) Schematic view of a viscoelastic slab incorporating inclusions, corresponding to the micro-inclusion technology. (On the right.) Microscope view of the actual inclusions in a slab (reproduced from [3]).

noise from any civilian maritime system, such as commercial ships, marine renewable energy systems, or more generally the exploitation of ocean resources, and the availability of related technical solutions is of increasing interest.

1.2. Frequency range of interest

Underwater acoustics cover a wide frequency range of interest. For example, the characterisation of sea bottom or the detection of objects on the sea floor generally involves systems operating with frequencies from a few kHz up to several hundreds of kHz, whereas long-range detection sonars use lower frequencies. The size order corresponding to the wavelength is that of the centimetre. Thus, the design or the choice of an acoustic coating will depend on the application and of the frequency range of interest.

1.3. Technology

On the technological aspect, these coatings generally consist in viscoelastic layers, a few centimetres thick, with some repartition of voids and other inclusions in the matrix.

The technology can be split into two main types: micro-inclusion technology consisting of micro-voids and/or other very small micro-inclusions (<1 mm) randomly distributed in a viscoelastic matrix, and macro-inclusion technology, which uses inclusions still smaller than the typical wavelength but on the same order of size (cm). The latter can itself be split into two categories:

- macro-inclusions randomly distributed in a viscoelastic matrix, which is the extension of the micro-inclusion technology where local resonances of the inclusions are observed in the frequency range of interest,
- Alberich-type coatings, consisting generally of macro-inclusions arranged periodically in a viscoelastic matrix. In this case, additional phenomena occur in relationship with the periodic arrangement of inclusions.

These different technologies can be used for the realisation of both absorbing and decoupling coatings, depending on the design.

In the micro-inclusion technology, the absorption or attenuation is obtained by incorporating micro-voids, generally in the form of micro-balloons with soft walls (Fig. 2). Besides, in order to obtain the desired performance for the coating, several layers of viscoelastic slabs with different properties or volume ratio of inclusions can be used. The presence of air inclusions, if any, renders the material dependent on hydrostatic pressure, which has to be taken into account for underwater applications [3,4]. In most current realisations, these inclusions are microscopic, but it would be possible to realise materials with larger inclusion sizes, allowing one to obtain acoustical effects at lower frequencies.

Alberich-type coatings generally use a periodic arrangement of inclusions in a viscoelastic matrix, either in two or three dimensions, as shown in Fig. 3. In most current realisations, there is only one layer of inclusions. However, it is possible to realise coatings formed with several layers. Some examples will be given in Section 3.

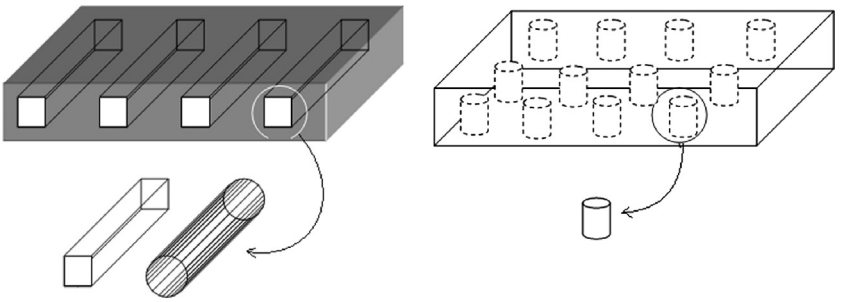

Fig. 3. Alberich coating made of inclusions equally spaced in a rubber layer: (on the left) using a 2D geometry or (on the right) a 3D geometry.

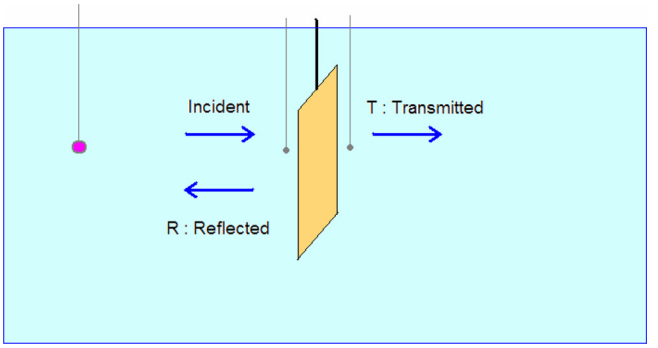

Fig. 4. (Colour online.) Schematic view of a test panel measurement in a water tank. Dots stand for transducers.

However, it should be noted that in case of presence of air in a soft material (such as polyurethane or rubber) the structure is deformable under hydrostatic pressure. Therefore, this structure is compressible and subject to geometry changes, causing changes of coating properties [5,6] related to a frequency shift of the resonances of the inclusions. This may be a problem for underwater applications where hydrostatic pressure is important.

Instead of using air or gas inclusions in the viscoelastic layer, it is possible to use materials such as steel or other metals. In that case, the advantage is a small influence of hydrostatic pressure. This type of inclusion can be considered to design and realise absorbing coatings, but is not well adapted for efficient decoupling coatings. The reason is that the efficiency of decoupling coatings is obtained if the dynamic stiffness of the coating is sufficiently low by comparison to water, and for that the incorporation of air or gas is necessary.

1.4. Characterisation

The commonly used method to determine the performance of an acoustic coating is the measurement of a test panel in a water tank (Fig. 4). Acoustic waves are generated in water using a transducer, generally in the form of sinusoidal signals with a time window. Hydrophones are placed on both sides of the test panels, in near field, to measure the acoustic pressure. A reference measurement without panel is done, then a measurement with test panel. Comparison allows determining reflection and transmission coefficients (both amplitude and phase) as a function of frequency, by varying the frequency of the emitted signal.

The measurement needs to be done with care, in particular to deal with the disturbances related to the finite size of the sample [7]. Besides, the use of special post-processing methods allows one to estimate the actual anechoic and decoupling performance [8].

2. Coatings composed of viscoelastic materials with micro-inclusions

2.1. Physical phenomena

Due to the random distribution of inclusions in a viscoelastic matrix, and assuming that both the inclusion size and the average distance between adjacent inclusions are small with respect to the wavelength, the coherent acoustic waves propagating in a micro-inclusion material can be characterised in the same way as for an isotropic elastic material, i.e. through an equivalent density ρ, longitudinal speed of sound c_L and transverse speed of sound c_T. Because of the behaviour of viscoelastic media, these speeds of sound are complex-valued and vary with frequency (and also with temperature). It should be noted that in the case of viscoelastic matrices without inclusions, c_T is low and c_L is close to sound speed in

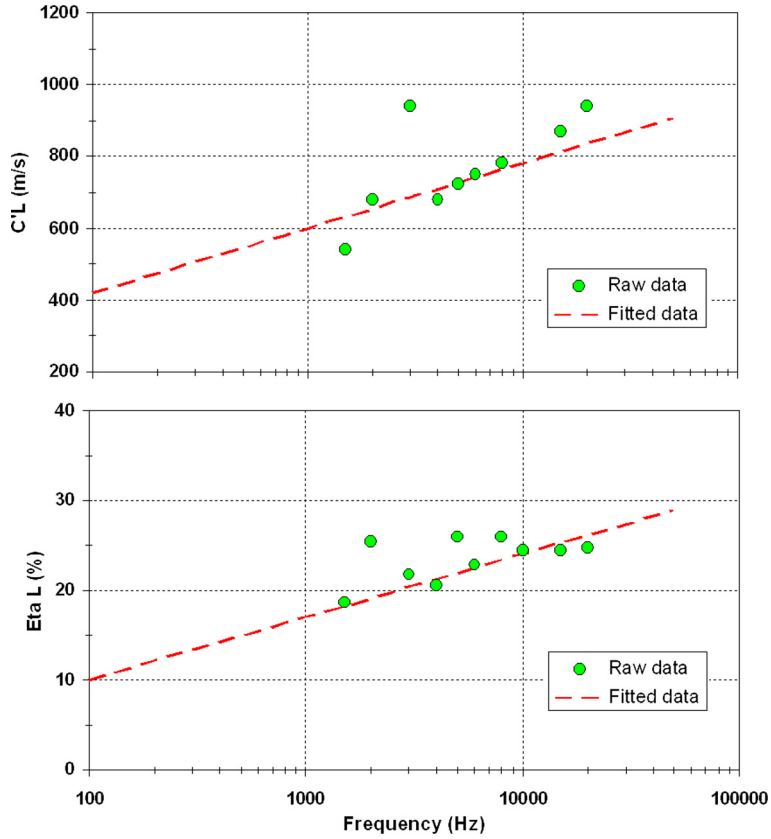

Fig. 5. (Colour online.) Evolution with frequency of longitudinal speed of sound (C'L) and dissipative part of it (EtaL) of a test anechoic material.

water, and that their density is also close to the one of water. As a consequence, a layer of viscoelastic material immersed in water is nearly acoustically transparent, without any significant absorbing or decoupling property.

The incorporation of air and/or other micro-inclusions in the viscoelastic matrix will alter significantly the acoustic properties of the latter. In the low-frequency domain, i.e. in the quasi-static regime for wavelengths much larger than the inclusions' size, the effective acoustic properties of the composite can be predicted by different models or theories, such as those of Kuster and Toksöz [9]. It is observed that the longitudinal speed of sound decreases and that the corresponding attenuation coefficient increases. Besides, the incorporation of heavy mineral micro-inclusions allows adjusting the density. Therefore, depending on the composition of the composite, it is possible to design materials with adequate anechoic and decoupling properties. As an example, Fig. 5 taken from [4] shows the evolution with frequency of the longitudinal speed of sound of a test anechoic material. In this figure c'_{L} represents the real part of $c_{\mathrm{L}} = \omega/k_{\mathrm{L}}$, where k_{L} is the longitudinal wavenumber and ω the circular frequency, and $\mathrm{Eta}_{\mathrm{L}}$ is the ratio of the imaginary part over the real part.

2.2. Recent developments

Some studies regarding micro-inclusion materials have dealt with the modelling of the influence of the walls of the micro-balloons and of hydrostatic pressure on the acoustic properties [3,10]. This topic is of continuing interest, as all phenomena are not yet properly described by the models.

Other recent studies have considered the case where the size of inclusions is no more negligible with respect to the wavelength and where local resonances of the inclusions in the matrix appear in the frequency range of interest. Consequently, quasi-static models are not applicable, and higher-order developments in multiple scattering theory must be taken into account. For example, in references [11] and [12], some composites made with a polyurethane matrix and either soft or rigid inclusions with sizes up to 1 mm have been studied. Predictive models for the effective speed of sound in the material and sound transmission through a layer in water have been developed and compared with experiments. As shown in Fig. 6, taken from reference [11], a variation of the transmission coefficient with frequency is directly related to the resonance of the inclusions in the matrix. The upper curve corresponds to the matrix only, for comparison. For the same concentration, the transmission coefficient with soft inclusions is much lower, the phenomenon being similar to the resonance of air bubble curtains in water [13].

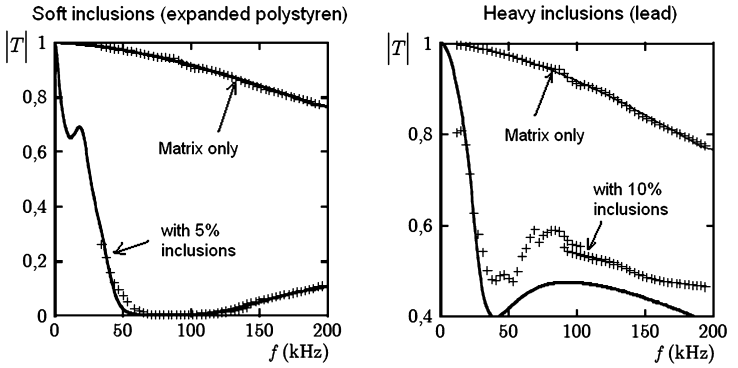

Fig. 6. Theoretical (solid lines) and experimental (crosses) transmission coefficient through a 15-mm-thick layer of polyurethane with inclusions. Left: 5% volume fraction of soft inclusions (2 mm diameter). Right: 10% volume fraction of rigid inclusions (1 mm in diameter).

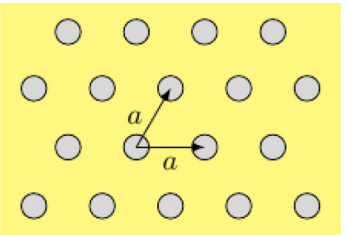

Fig. 7. (Colour online.) Representation of the 2D phononic crystal made of a triangular lattice of void/steel cylinders embedded in a matrix.

3. Acoustic coatings with macro-inclusions

Coatings made of periodic inclusions are known since World War Two, when a German submarine was coated with rubber panels with voids [5], introducing the now commonly used terminology “Alberich coatings”. This technology has considerably increased stealth and has been extensively studied since then [6,14–17].

3.1. Physical phenomena

In the case of classical decoupling materials, the presence of air inclusions in a relatively high volume ratio allows obtaining much lower acoustic impedance than water, a phenomenon which can be enhanced by the resonances. This property is adequate for the design of decoupling coatings.

Absorption mechanism in Alberich coatings is related to the resonance of the inclusions in the viscoelastic matrix, the latter being chosen with a high damping coefficient. In the case of short cylinders in a polymer matrix, the resonance mechanism related to a radial in-and-out motion coupled to a drum-like oscillation of the cover layer can increase significantly panel absorption [18]. In that case, the frequency range corresponding to strong attenuation is due to the resonance of the inclusion and is referred to as ‘hybridisation gap’. Another way to increase absorption is to use several layers, in order to benefit from the periodicity of the structure, commonly named Phononic Crystals (PC). Depending on the geometry of the inclusions, the materials and the type of the lattice (square, rectangular…), the dispersion curves, that represent the variations of the eigenfrequencies versus the wave number, may exhibit Bragg band gaps, i.e. frequency ranges where waves are strongly attenuated [19,20]. Indeed, for wavelengths comparable to the lattice constant, waves are evanescent inside the crystal due to interference effects, and the transmission spectrum is strongly attenuated in this specific frequency range.

In the following sections, we focus on phononic crystals and their periodical structure effects. We consider the cases of void or steel cylinders of infinite length embedded in a polyurethane material (Fig. 7). Thanks to judicious choices of cylinder diameter, periodicity, and lattice, a Bragg band gap is observed for void inclusions in the frequency range of the study. On the other hand, for the same geometry but with the void inclusions replaced by steel inclusions, we show that hybridisation gaps appear below a Bragg band gap. Moreover, this second structure is compatible with underwater pressure, contrary to the highly compressible void inclusions.

3.2. Results for void inclusions

The structure under study is a triangular lattice of cylindrical void inclusions embedded in a polymer matrix (Fig. 7). The matrix is a polyurethane material, whose properties are a density of 1.1, a longitudinal wave velocity $c_L = 1513$ m/s and a transverse wave velocity $c_T = 174$ m/s. The diameter of the cylinders is 1.9 mm and the spacing a is 10 mm. The structure is analysed using the finite-element method, with the help of the ATILA code [21]. Because the cylinders are supposed to be

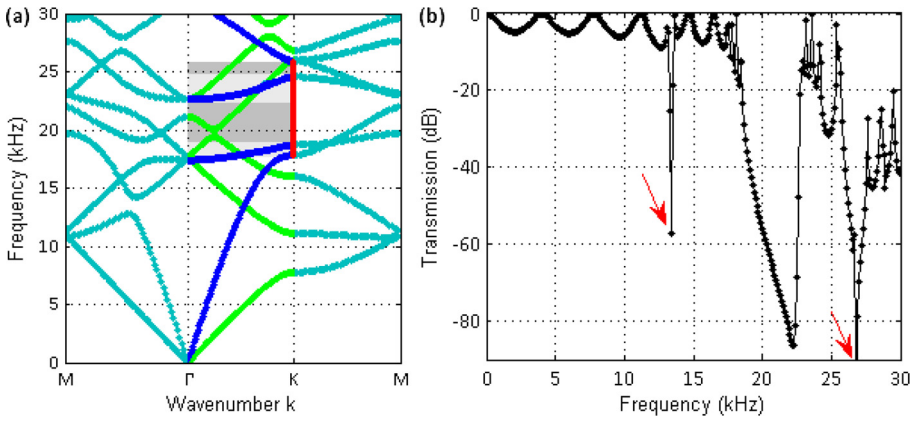

Fig. 8. (Colour online.) (a) Dispersion curves of the infinite crystal with void inclusions: for normal incidence, longitudinal modes (in dark grey/blue) are distinguished from transverse modes (in light grey/green). (b) Transmission spectrum of a 7-layer crystal under normal incidence. Red arrows indicate the position of local phenomena effects.

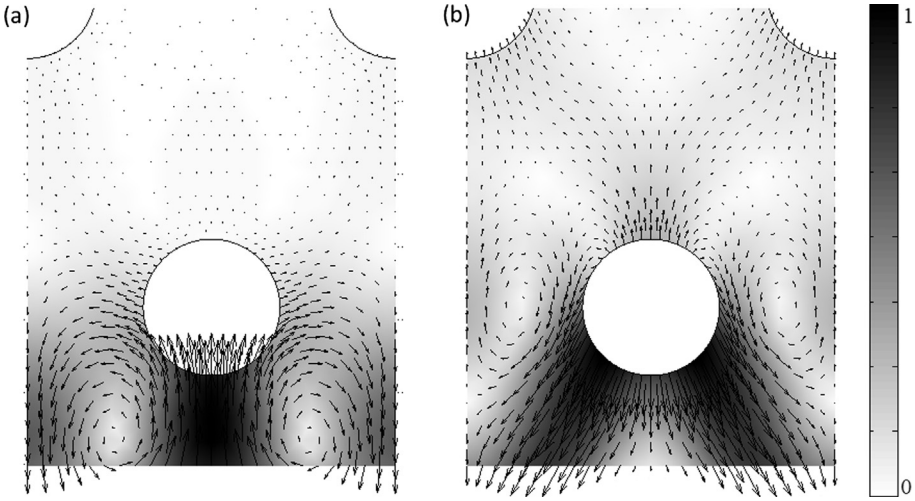

Fig. 9. Amplitude of the displacement fields near interface when the incident wave comes from the bottom at (a) $f = 13.4$ kHz and (b) $f = 26.8$ kHz. Arrow size and orientation indicate the total displacement magnitude and displacement vector orientation, respectively. The displacement magnitude is also shown as a grey scale map, for clarity.

infinite in length, a two-dimensional mesh is used, with a plane strain condition. In a first step, the infinite PC is studied in order to calculate the dispersion curves. In that case, only one unit cell of the PC is meshed and specific periodic conditions are applied on the boundaries of the unit cell [22]. The calculation gives, for each wavenumber in the first Brillouin zone, the corresponding eigenfrequencies, shown in Fig. 8a. Solutions corresponding to longitudinal and transverse modes are distinguished. Note that we can safely remove the transverse modes from the picture, since we only consider operation under normal incidence and, in this case, they cannot couple with the incident pressure waves in the fluid region. We can see that there is no solution for the longitudinal wavenumber at normal incidence in the [18–26 kHz] frequency range, apart from two narrow pass-bands around 18 and 23 kHz related to resonant modes of the void inclusions. This frequency range corresponds to the partial Bragg band gap for propagation along the Γ K direction. Due to the periodic distribution of inclusions, the waves at these frequencies cannot propagate through the infinite structure.

We now consider a panel made of seven layers of this structure, surrounded by water, neglecting losses in the elastic matrix. The transmission spectrum, shown in Fig. 8b, clearly confirms the band-gap effect. Two sharp dips are indicated by arrows. They are due to local phenomena around the panel interfaces. For these frequencies, the incoming wave strongly couples with a resonant interface mode. Therefore, displacement fields remain localised at the interface and vanish rapidly inside the panel, as shown in Fig. 9.

These mechanisms will be studied later in Section 3.4. If the viscous losses in the matrix are taken into account, the transmission spectrum is smoothed (Fig. 10), but the band gap is still pronounced. It can be noted that the dips related to interface effects become hardly distinguishable. Moreover, we see that the transmission coefficient level remains low at high frequencies, even outside of band gaps because of viscous effects.

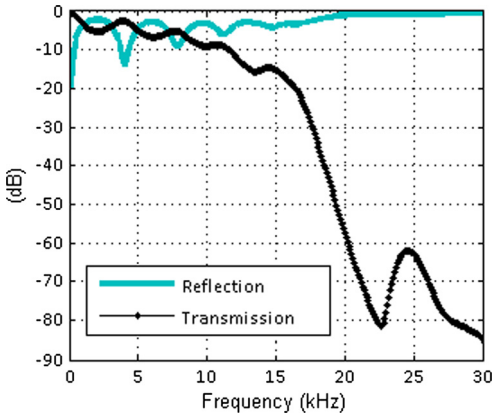

Fig. 10. (Colour online.) Transmission and reflection spectra of a 7-layer crystal with void inclusions considering viscoelasticity.

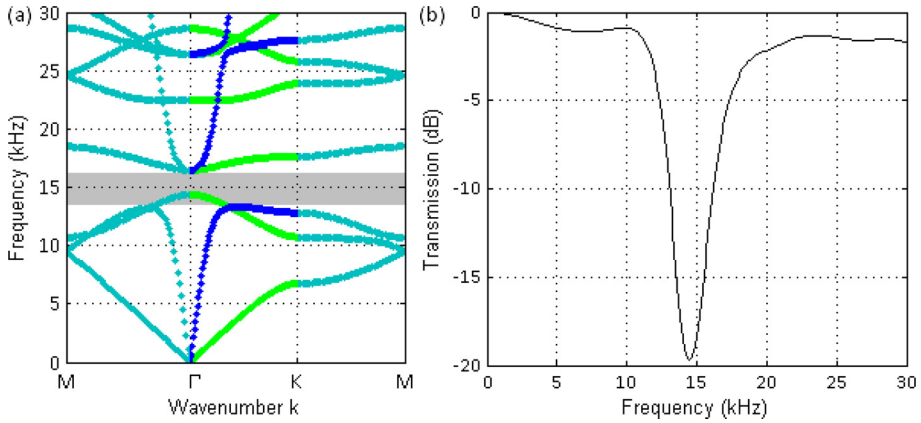

Fig. 11. (Colour online.) (a) Dispersion curves of the infinite with steel inclusions: for normal incidence, longitudinal modes (in dark blue) are distinguished from transverse modes (in light green). The grey band represents the hybridisation gap. (b) Transmission spectrum for a 5-layer crystal.

3.3. Results for rigid inclusions

The structure is kept unchanged except for the inclusion material, as now they are made of steel. As previously, the first step is to calculate the dispersion curves of this phononic crystal. Results are presented in Fig. 11a. We can see that, if transverse modes are discarded, there are no solutions in the 14–16-kHz frequency range. Displacement maps for the modes at the Γ and K points of the band diagrams surrounding this gap (Fig. 12) clearly show that a resonant oscillation mode of the steel rods is present in this frequency range. It hybridises with the mode propagating mainly through the elastic matrix to create the gap, which can thus be labelled as a "hybridisation gap". Indeed, the Bragg band gap associated with this periodic structure occurs at much higher frequencies (around 80–90 kHz). Considering now a panel made of five layers of PC surrounded by water, the transmission coefficient (Fig. 11b) calculated using the finite element method confirms that the transmission is strongly reduced in the 14–16-kHz frequency range. A 5-layer structure corresponds to a crystal thickness of 43.3 mm. It is inside a panel of total thickness equal to 61 mm. We can notice that the lattice constant a is ten times shorter than the wavelength in the polyurethane at 15 kHz (101 mm).

3.4. Perspectives

Periodic structures with steel inclusions exhibit a strong resonance-related band gap. However, its width is relatively narrow. This band gap can be enlarged with the help of interface modes. Indeed, periodic arrangements of steel inclusions show specific resonance effects near fluid interfaces.

In order to illustrate this phenomenon, let us consider panel A presented in Fig. 13. It contains seven layers of a PC made of a triangular arrangement of steel cylinders. The interfaces delimiting the panel are close to the first and the last rows of inclusions. The transmission spectrum of the panel surrounded by water is presented in Fig. 15. Structure A is then split into structures B and C. B does not contain the first and the last rows of inclusions, whereas C only contains those two rows. Fig. 15 presents the transmission coefficients for panels B and C. As expected, waves are attenuated in panels A and B in the 14–16-kHz frequency range, due to the hybridisation band gap. Case C considers inclusions near interfaces exclusively.

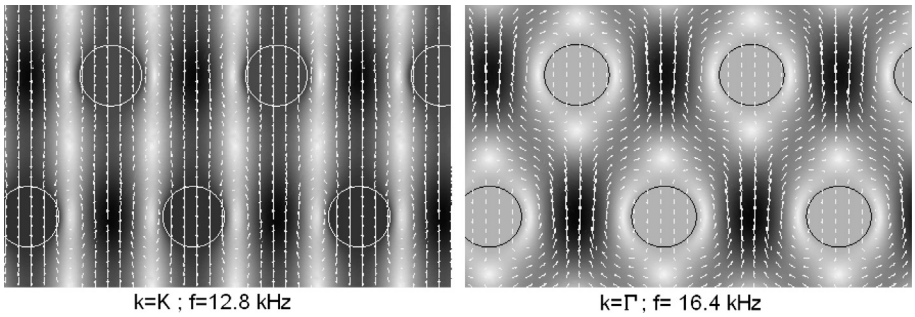

Fig. 12. Displacement field for longitudinal modes around the hybridisation gap of the crystal with steel inclusions. The same arrow/grey scale representation as in Fig. 9 is used.

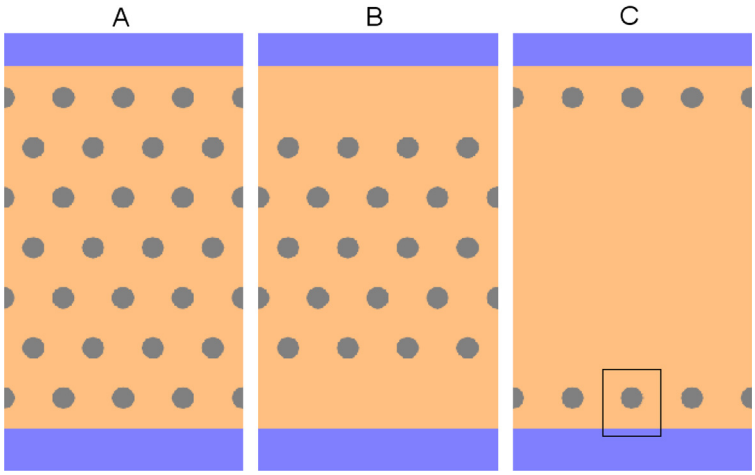

Fig. 13. (Colour online.) Schematic of different cases of inclusions (in grey) embedded in the matrix (in orange) surrounded by water (in blue). The black rectangle in C indicates the location of the field maps shown in Fig. 14.

In the most simple hybridisation scheme, it is assumed that the inclusion resonance does not depend on its surroundings, and therefore we should see a transmission dip centred on 15 kHz, even for panel *C*. However, the displacement maps of Fig. 12 clearly show that the resonant mode involved here is strongly localised in the matrix (the steel cylinders are much denser and almost incompressible with respect to the polymer matrix). In this case, resonance is greatly influenced by the presence or absence of neighbouring rows of inclusions. This is evidenced in the transmission spectrum by a large frequency shift of the main dip, from 15 kHz to 12.3 kHz, along with the apparition of a secondary dip around 21.4 kHz. The displacement maps in the first row of inclusions at these two frequencies (Fig. 14) allow us to clarify this behaviour. At the first frequency, the map bears a strong similarity with the mode in the infinite crystal (as shown in the second graph of Fig. 12 for instance), but modified by the presence of an interface on one side and a matrix with no inclusion on the other side. At the second frequency, we observe that displacement fields are mainly localised between the matrix interface and the first row of inclusions. Note that this second resonance is completely absent from the transmission spectrum of panel *B*, which does not possess inclusions located close to the interface, whereas it is clearly visible in the spectrum of panel *A*. In summary, the transmission spectrum of panel *A* is the result of three effects, namely (a) the hybridisation with an inclusion resonance, (b) the periodic arrangement of those inclusions (which strongly modifies the hybridisation effect), and (c) the presence of resonant interface modes.

The displacement fields presented in Fig. 14 suggest that frequencies and resonance amplitude can be tuned by changing the geometry for the first and the last layers of inclusions. Therefore, a parametric study has been performed in order to improve the transmission coefficient of the panel. Fig. 16 presents the improved configuration, where the inclusions near interfaces are larger and located further apart. In this case, the first resonance frequency is outside the band gap (11.3 kHz) and strong enough to reduce significantly the transmission coefficient (Fig. 17). The second resonance frequency (21.8 kHz) also helps to enlarge the frequency range where transmission is lower than −5 dB.

4. Conclusions

The presence of inclusions in a viscoelastic matrix, either randomly or periodically distributed, alters strongly its acoustic properties, which allows the design of anechoic or decoupling coatings for underwater acoustics applications.

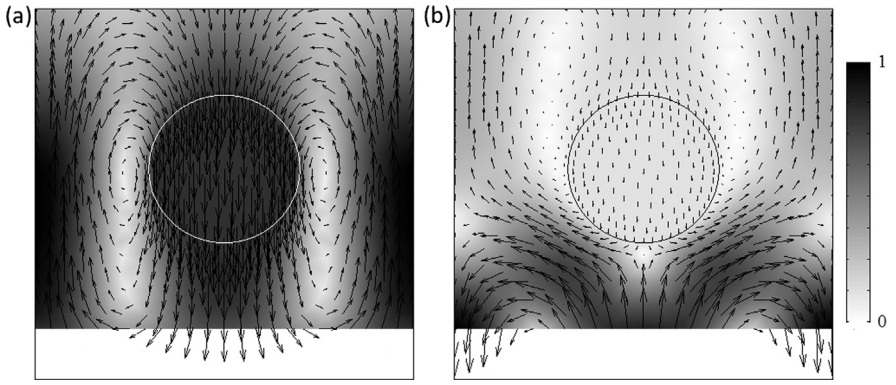

Fig. 14. Displacement fields close to the front interface for panel *C* under normal incidence at (a) 12.3 kHz and (b) 21.4 kHz, with the same arrow/grey scale representation as in Fig. 9.

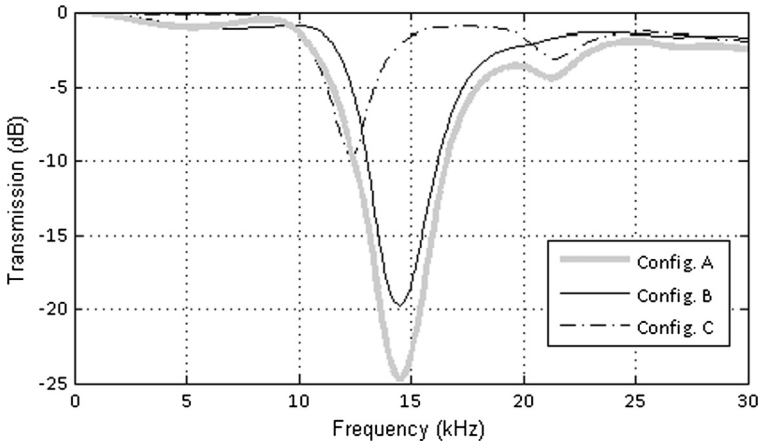

Fig. 15. Transmission spectra for cases from Fig. 9.

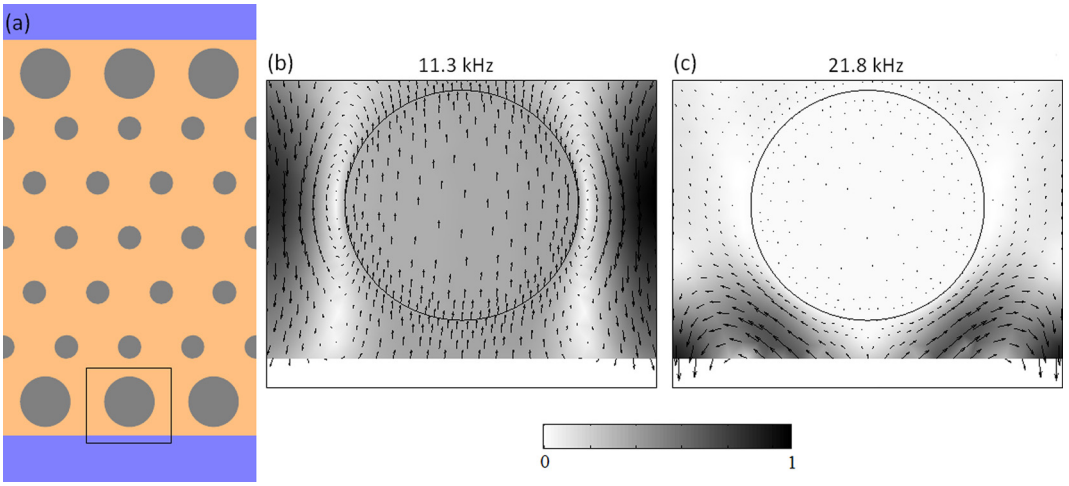

Fig. 16. (Colour online.) (a) Schematic view of the optimised structure. The black rectangle indicates the location of the field maps in the first row under normal incidence shown in (b) and (c) at 11.3 and 21.8 kHz respectively, with the same arrow/grey-scale representation as in Fig. 9.

In the micro-inclusion case, the material can be represented by equivalent properties. When frequency increases, acoustical effects related to the resonances of the inclusions in the matrix appear. In particular, by using a few percent of air inclusions, low transmission coefficients can be obtained in a wide frequency range.

In the macro-inclusion case, different phenomena appear. The analysis can be conducted using finite element models, for example here with the ATILA code. First, the classical PC pass-band or stop-band effects appear, in relationship with

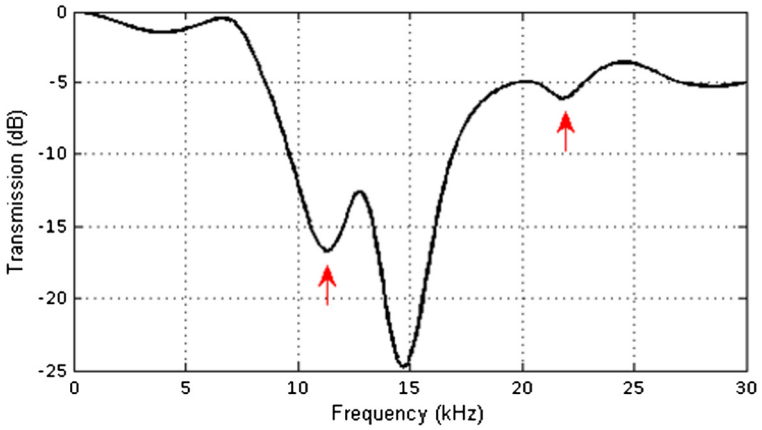

Fig. 17. (Colour online.) Transmission spectrum for the optimised structure.

the geometry (periodic arrangement of inclusions). A second class of phenomena is related to the resonances of inclusions in the matrix, allowing obtaining transmission effects at lower frequencies. In this paper, we have shown that additional effects can be obtained with particular arrangements of inclusions and interface effects. Several examples and the result from an optimisation study have been shown in the case of steel inclusions in a polyurethane matrix. It should also be noted that, unlike the use of air inclusions, the use of rigid inclusions allows the design of materials whose characteristics are not affected by hydrostatic pressure. It has also been shown that in the case where the material of the matrix is lossy, some effects are less visible. In any case, it is important to take into account the lossy character of this type of material.

The variability of acoustic phenomena with geometry, arrangement of layers, matrix properties and type of inclusions opens wide possibilities for the design of acoustic coatings adapted to different applications. This is a challenging research topic for the future.

Acknowledgement

This study has been supported by DGA (Direction Générale de l'Armement, France) via a Ph.D. grant with DCNS Research.

References

[1] C. Audoly, Acoustic characterisation of anechoic or decoupling coatings taking into account the supporting hull, in: RINA Warship Conference, Naval Submarines and UUV, Bath, UK, 2011, pp. 29–30.
[2] Marine Strategy Framework Directive, Task Group 11 Report, Underwater noise and other forms of energy, Prepared under the Administrative Arrangement between JRC and DG ENV (no 31210-2009/2010), the Memorandum of Understanding between the European Commission and ICES managed by DG MARE, and JRC's own institutional funding Walree, 2010.
[3] S. Beretti, Réponse acoustique d'élastomère micro-inclusionnaires soumis à la pression d'immersion, in: 10e Congrès français d'acoustique, 2010.
[4] C. Audoly, Evaluation of sound velocity inside underwater acoustic materials using test panel acoustic measurements, in: 10th Anglo–French Physical Acoustics Conference, J. Phys. Conf. Ser. 353 (2012) 012004.
[5] E. Meyer, W. Kuhl, H. Oberst, E. Skudrzyk, K. Tamm, Sound absorption and sound absorbers in water (dynamic properties of rubber and rubberlike substances in the acoustic frequency region), in: Report NavShips 900, vol. 1, Department of the Navy, Washington, DC, USA, 1950, p. 164.
[6] G. Gaunaurd, One dimensional model for acoustic absorption in a viscoelastic medium containing short cylindrical cavities, J. Acoust. Soc. Amer. 62 (2) (1977) 298.
[7] C. Granger, C. Audoly, P. Méresse, G. Haw, Mesure des coefficients de réflexion et de transmission de panneaux en cuve acoustique – étude comparative de différentes méthodes, in: Congrès français d'acoustique, Poitiers, France, 2014.
[8] C. Audoly, Determination of efficiency of anechoic or decoupling hull coatings using water tank acoustic measurements, in: Congrès français d'acoustique, Nantes, France, 2012.
[9] G.T. Kuster, M.N. Toksöz, Velocity and attenuation of seismic waves in two-phase media: theoretical formulations, Geophysics 39 (5) (1974) 587–606.
[10] A.M. Baird, F.H. Kerr, D.J. Townend, Wave propagation in a viscoelastic medium containing fluid-filled microspheres, J. Acoust. Soc. Amer. 105 (3) (1999) 1527–1538.
[11] G. Lepert, Étude des interactions élasto-acoustiques dans des métamatériaux formés d'inclusions résonnantes réparties aléatoirement, Ph.D. thesis, Université Bordeaux-1, 2013.
[12] G. Lepert, C. Aristégui, O. Poncelet, T. Brunet, C. Audoly, P. Parneix, Recovery of the effective wavenumber and dynamical mass density for materials with inclusions, in: Congrès français d'acoustique, Nantes, France, 2012.
[13] G. Gaunaurd, Resonance theory of bubbly liquids, J. Acoust. Soc. Amer. 69 (2) (1981) 362–370.
[14] R. Lane, Absorption mechanisms for waterborne sound in Alberich anechoic layers, Ultrasonics 19 (1981) 28–30.
[15] A.-C. Hladky-Hennion, J.N. Decarpigny, Analysis of the scattering of a plane acoustic wave by a doubly periodic structure using the finite element method: application to Alberich anechoic coatings, J. Acoust. Soc. Amer. 90 (6) (1991) 3356.
[16] S. Ivansson, Sound absorption by viscoelastic coatings with periodically distributed cavities, J. Acoust. Soc. Amer. 119 (6) (2006) 3558.
[17] S. Ivansson, Anechoic coatings obtained from two- and three-dimensional monopole resonance diffraction gratings, J. Acoust. Soc. Amer. 131 (4) (2012) 2622.

[18] G. Gaunaurd, Comments on 'Absorption mechanisms for waterborne sound in Alberich anechoic layers', Ultrasonics 23 (2) (1985) 90–91.
[19] M.S. Kushwaha, P. Halevi, L. Dobrzynsky, B. Djafari-Rouhani, Acoustic band structure of periodic elastic composites, Phys. Rev. Lett. 71 (13) (1993) 2022.
[20] M.S. Kushwaha, P. Halevi, G. Martinez, L. Dobrzynsky, B. Djafari-Rouhani, Theory of acoustic band structure of periodic elastic composites, Phys. Rev. B 49 (4) (1994).
[21] ATILA, Finite-element software package for the analysis of 2D & 3D structures based on smart materials, version 6.0.2, User's manual, 2010.
[22] P. Langlet, A.-C. Hladky-Hennion, J.-N. Decarpigny, Analysis of the propagation of plane acoustic waves in passive periodic materials using the finite element method, J. Acoust. Soc. Amer. 98 (5) (1995) 2792.